Available online at www.sciencedirect.com
SCIENCE DIRECT
Thermochimica Acta 444 (2006) 195–200
thermochimica acta
www.elsevier.com/locate/tca

Short communication

Phase polymorphism of $[Zn(DMSO)_6](ClO_4)_2$ studied by differential scanning calorimetry

A. Migdał-Mikuli *, E. Szostak

Department of Chemical Physics, Faculty of Chemistry, Jagiellonian University, ulica Ingardena 3, 30-060 Kraków, Poland

Received 23 January 2006; accepted 3 February 2006
Available online 11 April 2006

Abstract

Four solid phases of $[Zn(DMSO)_6](ClO_4)_2$ have been detected by differential scanning calorimetry (DSC). Specifically, the phase transitions were detected between: metastable phase KII ↔ supercooled phase K0 at $T^h_{C3} = 315$ K, stable phase KIb ↔ stable phase KIa at $T^h_{C2} = 341$ K, stable phase KIa ↔ stable phase K0 at $T^h_{C1} = 355$ K. At $T_{m2} = 389$ K crystals partially and at $T_{m1} = 465$ K completely melts. From the entropy change values it was concluded that the phases: K0 and K0′ are the orientationally dynamically disordered phases, so called ODDIC crystals, and phases KIa, KIb and metastable KII are dynamically ordered but with some degree of positional disorder.

Keywords: Hexadimethylsulphoxidezinc(II) chlorate(VII); Phase transitions; Two-stage melting; ODDIC; DSC

1. Introduction

Hexadimethylsulphoxidezinc(II) chlorate(VII) (called later HZnC) crystallizes in a trigonal system at ambient temperature and belongs to the P31c space group (no. 159) [1,2]. These crystals form a primitive lattice with a number of molecules in an elementary cell $Z = 2$. The lattice parameters are $a = 12.006$ Å and $c = 12.578$ Å [1,2]. The crystalline structure of the title compound consists of two kinds of complex ions: $[Zn((CH_3)_2SO)_6]^{2+}$ and ClO_4^-. The $[Zn((CH_3)_2SO)_6]^{2+}$ cation is built like a slightly distorted octahedron. The zinc atom is surrounded octahedrally by six oxygen atoms coming from the dimethylsulphoxide (referred to as DMSO in short) ligands [3]. The average length of bonds between atoms of zinc and oxygen is 2.110 Å. The DMSO ligands are built like C_{2v} pyramids. The average distances between S–O and S–C atoms are 1.494 and 1.790 Å, respectively. There are two kinds of ClO_4^- tetrahedral ions in elementary cell. Each of it have different grade of disorder [1,2].

We have recently investigated, by differential scanning calorimetry (DSC), the polymorphism of the three following compounds: $[Cd(DMSO)_6](ClO_4)_2$ (called HCdC) [4], $[Co(DMSO)_6](ClO_4)_2$ (called HCoC) [5] and $[Mn(DMSO)_6](ClO_4)_2$ (called HMnC) [6]. We found that at the temperature range of 100–450 K HCdC and HCoC have five and HMnC six solid phases. In all these compounds two phases are metastable and the remaining phases are stable. The high temperature stable phases of these compounds are orientationally dynamically disordered and can be easily supercooled. We found also the melting points of these compounds. The purpose of this work was to discover the polymorphism of HZnC in the temperature range of 153–513 K using the differential scanning calorimetry method (DSC).

2. Experimental

2.1. Sample preparation

A few grams of $[Zn(H_2O)_6](ClO_4)_2$ were dissolved while being slowly heated up in DMSO of high chemical purity, which was previously additionally purified by vacuum distillation at low pressure and next was dehydrated by shaking with anhydrous $CaCl_2$, according to requirements presented in [7]. This solution was then chilled and the precipitated crystals of HZnC were filtered and washed with acetone. They were then dried in desiccator over phosphorous pentaoxide for a few hours. After

* Corresponding author. Tel.: +48 12 633 6377x2256; fax: +48 12 634 0515.
E-mail addresses: migdalmi@chemia.uj.edu.pl (A. Migdał-Mikuli), szostak@chemia.uj.edu.pl (E. Szostak).

0040-6031/$ – see front matter © 2006 Elsevier B.V. All rights reserved.
doi:10.1016/j.tca.2006.02.005

desiccation, they were put in a sealed vessel and stored in desiccator with barium oxide as a desiccant.

To check the chemical composition of the synthesized HZnC, the percentage content of zinc ions was checked using a complexometric method, with a solution of the sodium salt of ethylenediaminetetraacetic acid (EDTA) as a titrant. The theoretical content of zinc equaled 8.92% and its content found by the titration analysis amounted to $8.81 \pm 0.18\%$. The content of carbon and hydrogen in the DMSO ligands was determined using elementary analysis on a EURO EA 3000 apparatus. For carbon atoms, the difference between the theoretical value (19.66%) and the test value ($19.71 \pm 0.02\%$) did not exceed 0.1%. For hydrogen atoms, the theoretical value was 4.95% and the test value was $4.83 \pm 0.09\%$. Therefore, the elementary analysis of the title compound confirmed presence of the stoichiometric number of six DMSO molecules in the complex cation.

2.2. Sample identification and characteristics

In order to further identify the title compound, its infrared absorption spectra (FT-FIR and FT-MIR) and its Raman spectrum (FT-RS) were recorded at ambient temperature. The FT-FIR and FT-MIR spectra were obtained using Digilab FTS-14 and EQUINOX-55 Bruker Fourier transform infrared spectrometers, respectively, with a resolution of $2\,cm^{-1}$. For a powder sample, suspended in Apiezon grease, the FT-FIR spectrum was recorded using polyethylene and silicon windows. The FT-MIR spectrum was recorded for a sample suspended in Nujol between the KBr pellets. The FT-RS spectrum was recorded using a Bio-Rad spectrometer with a YAG neodymium laser ($\lambda = 1064$ nm) at 10–4000 cm^{-1} with resolution of $4\,cm^{-1}$. Fig. 1 presents a comparison of the infrared and Raman spectra and Table 1 contains a list of the obtained and literature data [3,8,9] of band frequencies and their assignments for HZnC. These data are submitted as supplementary data files and appear in the electronic version. They in addition to chemical analysis identify the investigated compound as $[Zn((CH_3)_2SO)_6](ClO_4)_2$.

Thermal analysis of the examined compound was made in order to enable further verification of its composition. The thermogravimetric (TG) measurements and simultaneous differential thermal analysis (DTA) were performed using a Mettler Toledo TGA/SDTA 851^e apparatus. A sample weighing 4.1705 mg was placed in a 150 μl Pt/Rh crucible. The TG measurements were made in a flow of argon (80 ml/min) from 303 K up to 420 K at a constant heating rate of 2 K/min. The simultaneous evolved gas analysis (SEGA), with on-line quadrupole mass spectrometer (QMS) using a Balzer GSD 300T apparatus, were also registered. The temperature was measured by a Pt–Pt/Rh thermocouple with the accuracy of ±0.5 K. The TG measurements of HZnC proved that during the heating of sample from 303 K up to 370 K (in a flow of argon) the sample does not lose more than ca. 2% of its initial mass. During heating up to 420 K the sample loses 10.58% of its initial mass and converts into the $[Zn(DMSO)_5](ClO_4)_2$ complex.

To sum up, the FT-RS, FT-FIR, FT-MIR spectra, chemical and thermal analysis (TG + QMS and SDTA) have jointly certified proper composition and the purity of the examined compound.

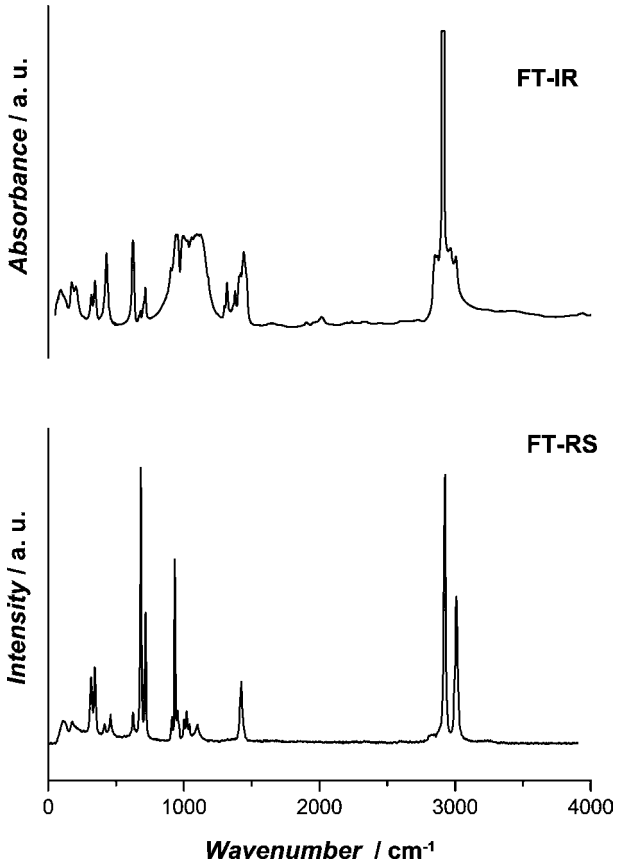

Fig. 1. Comparison of the Fourier transform infrared (FT-FIR and FT-MIR) and Raman scattering (FT-RS) spectra of $[Zn(DMSO)_6](ClO_4)_2$.

2.3. Heat flow measurements

The DSC measurements of HZnC were made using two types of DSC apparatus: the first one was a Perkin-Elmer PYRIS 1 DSC apparatus on which four samples were investigated in the temperature range of 153–420 K. The weight of these samples was, respectively: 16.96 mg (sample *a*), 17.83 mg (sample *b*) and 17.94 mg (sample *c*). The experimental details were the same as published in [10]. The second one was a Mettler Toledo DSC 821e apparatus used in the temperature range of 283–513 K. The weight of the sample was 28.34 mg (sample *d*).

3. Results and discussion

The temperature dependence of the difference of the thermal power supplied to the two calorimeters (the so called thermal stream), in short named the DSC curve or thermogram, was obtained for each of four samples of HZnC: *a*, *b*, *c* and *d* at different scanning rates and at initial and final heating and cooling conditions. The samples masses were chosen to check if the observed anomalies on DSC curves depend on the sample weight. The thermodynamic parameters of the detected phase transitions are given in Table 2. Samples without any "thermal history" are at room temperature in a crystalline state called KIb phase.

Table 1
The list of band positions of the Raman and infrared spectra of solid $[Zn(DMSO)_6](ClO_4)_2$ at room temperature

Frequencies (cm^{-1})							Assignment
$[Zn(DMSO)_6](ClO_4)_2$					DMSO[8,9]		
RS			IR		RS	IR	
This work	[3]	This work in KBr pellet	This work	[3]			
70 sh			71 w[a]				ν_L(lattice)
81 sh			85 w[a]				ν_L(lattice)
94 sh			94 w[a]				ν_L(lattice)
117 m			119 w[a]				ν_L(lattice)
176 m	176 w		174 m[a]	178 w			ν_d(ZnO)
206 sh			205 m[a]	192 w			ν_d(ZnO)
315 st	317 st				313 m	313 w	δ_{as}(CSC)
345 st	345 st		318 m[a]	321 w	338 m	338 m	δ_{as}(CSO)
			345 m[a]	368 w	388 m	381 m	δ_s(CSO)
417 w	416 w						ν_s(ZnO)
			429 m[a]	431 m			ν_{as}(ZnO)
459 m	460 m						δ_d(OClO)E
625 m	626 m	631 st	625 st[b]	621 vst			δ_d(OClO)F_2
			669 vw[b]			612 sh	ν_s(CS)
682 vst	683 vst	674 w	679 w[b]	660 vw	663 vst	663 m	ν_s(CS)
717 st	717 st	705 m	717 m[b]	694 w	700 m	700 st	ν_{as}(CS)
912 m	912 m	900 w	902 w[b]		900 vw	900 w	ρ(CH3)
933 st	935 vst	937 sh					ν_s(ClO)A1
			940 st[b]		925 vw	931 m	ρ(CH3)
953 m	954 m	954 st	952 st[b]	948 m	954 w	955 st	ρ(CH3)
1001 m	1003 m	999 w	997 br[b]				ρ(CH3)
1020 m	1021 st	1026 vst	1028 w[b]	1015 m			ν_s(SO)
1041 m	1042 m	1051 sh			1050 m	1050 vst	ν_s(SO)
			1057 w[b]				ν_d(ClO)F2
1100 m	1102 m	1103 sh	1099 br[b]	1100 w			ν_d(ClO)F2
		1121 st	1124 br[b]				ν_d(ClO)F2
		1180 vw	1179 sh[b]				
	1325 vw	1294 vw	1298 w[b]	1303 vw		1303 m	δ_s(HCH)
		1313 m	1318 m[b]		1313 w		δ_s(HCH)
		1344 vw	1377 st[b]				δ_{as}(HCH)
1424 st	1425 vst	1406 m	1408 sh[b]	1412 m		1404 st	δ_{as}(HCH)
		1435 m	1441 vst[b]		1425 m	1440 st	δa_s(HCH)
2809 vw		2854 w	2850 st[b]		2885 br	2825 br	ν_s(CH)
2850 vw		2899 sh	2872 sh[b]	2900 vw			ν_s(CH)
2926 vst		2915 m	2912 vst[b]		2913 vst	2910 st	ν_s(CH)
			2965 st[b]	2978 vw			ν_s(CH)
3008 st		2999 m	3007 st[b]		2998 m	2998 st	ν_{as}(CH)

vw, very weak; w, weak; sh, shoulder; m, medium; st, strong; vst, very strong; br, broad.
[a] In Apiezon.
[b] In Nujol.

The measurements on sample *a* were started by cooling the sample from room temperature (RT) to 153 K, holding it at this temperature for l min, then heating the sample up to 298 K. There was no anomaly on the DSC curves obtained at first cooling and at subsequent heating the sample *a* with a scanning rate of 20 K/min, thus these curves are not presented here. While heating sample *a*, being initially in the KIb phase, with a scanning rate of 20 K/min, from 298 to 370 K, the phase transition into

Table 2
Thermodynamics parameters of the detected phase transitions (on heating and cooling) of $[Zn(DMSO)_6](ClO_4)_2$

At heating					At cooling			
Phase transition		T_c (K)	ΔH (kJ mol^{-1})	ΔS (J mol^{-1} K^{-1})		T_c (K)	ΔH (kJ mol^{-1})	ΔS (J mol^{-1} K^{-1})
L0 → liquid	T_{m1}	456 ± 1	21.42 ± 0.82	47.0 ± 2.1				
K0 → L0	T_{m2}	389 ± 1	7.63 ± 0.23	19.6 ± 0.6	T^c_{m2}	386 ± 1	7.48 ± 0.14	19.4 ± 0.4
K0 → KIa	T^h_{C1}	355 ± 1	25.33 ± 0.69	71.4 ± 1.9				
KIa → KIb	T^h_{C2}	341 ± 1	2.37 ± 0.30	7.0 ± 0.9				
K0′ → KII	T^h_{C3}	315 ± 1	21.31 ± 3.15	67.7 ± 10.3	T^c_{C3}	309 ± 1	18.80 ± 5.62	60.8 ± 18.2

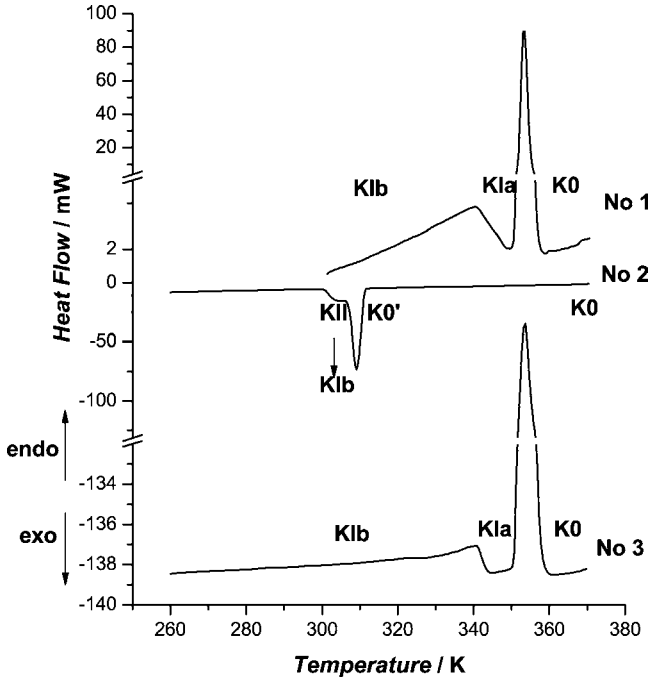

Fig. 2. Differential scanning calorimetry (DSC) curves obtained during heating from 298 to 370 K (curve no. 1), during cooling from 370 to 260 K (curve no. 2) with a scanning rate of 20 K/min and during heating from 260 to 370 K (curve no. 3) of $[Zn(DMSO)_6](ClO_4)_2$ with a scanning rate of 30 K/min. Sample $a = 16.96$ mg.

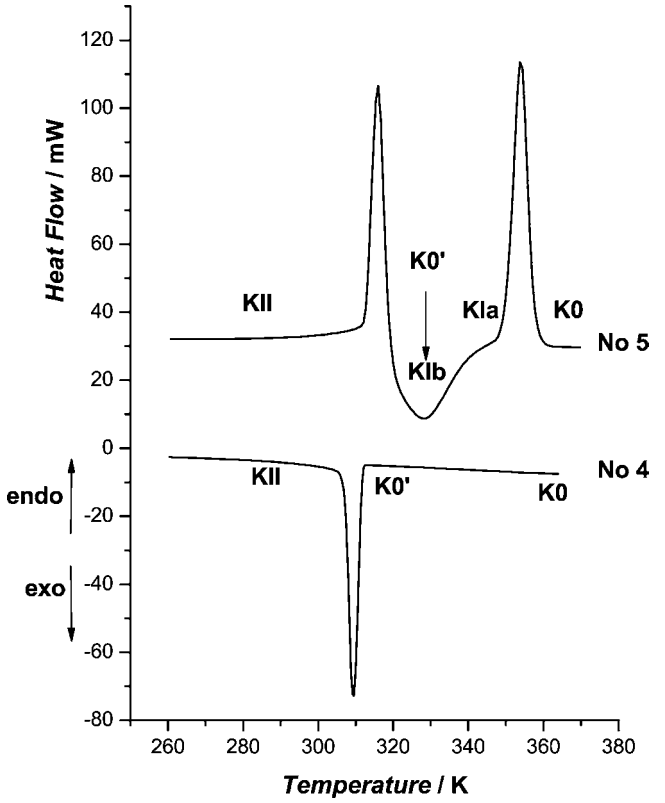

Fig. 3. DSC curves obtained for $[Zn(DMSO)_6](ClO_4)_2$ during cooling from 370 to 260 K (curve no. 4) with a scanning rate 30 K/min and during heating at 260–370 K (curve no. 5) with a scanning rate of 40 K/min. Sample $b = 17.83$ mg.

intermediate phase which was named KIa can be observed at $T^{h}_{C2} = 341$ K, as can be seen in Fig. 2 (there is a small anomaly on the DSC curve no. 1). Phase KIa next transforms at $T^{h}_{C1} = 355$ K into the high temperature phase, named K0, that is manifested as a big anomaly on the same curve no. 1. While cooling sample a from 370 to 260 K the K0 phase is strongly supercooled till 309 K when it goes into a metastable phase named KII, that is connected with a big anomaly on the DSC curve no. 2. On further cooling, at ca. 304 K the metastable KII phase transforms exothermically into the stable KIb phase, that is manifested in a small anomaly on the DSC curve no. 2 (see Fig. 2). Next heating of sample a with a scanning rate of 30 K/min gives the DSC curve no. 3 which is nearly identical to the curve no. 1. On the DSC curve no. 3 we can see one small anomaly at T^{h}_{C2}, connected with the phase transition stable phase KIb → stable phase KIa and one major anomaly at T^{h}_{C1}, connected with the phase transition stable phase KIa → stable phase K0.

Cooling the new sample (sample b) from 370 K down to 260 K, with a scanning rate 30 K/min, can cause transformation of the whole sample at ca. 309 K into a metastable phase KII, as can be seen in Fig. 3 (DSC curve no. 4). This phase transition is connected with a big anomaly on the DSC curve (see Table 2). Heating sample b with a scanning rate of 40 K/min gives the DSC curve no. 5 presented in Fig. 3. The sample, which was in the metastable phase KII, transforms at $T^{h}_{C3} = 312$ K in an endothermic process, that is connected with a big and sharp anomaly on the DSC curve, into the supercooled phase K0 (named K0′). At a slightly higher temperature the phase K0′ converts, in the exothermic process, to the stable phase KIb. We believe that this process is like a crystallization [11] from phase K0′ to the more stable phase KIb. When the heating of the sample is continued, the phase transition occurs from phase KIb to phase KIa, finally the stable phase KIa endothermically converts at $T^{h}_{C1} = 355$ K into the stable phase K0 (big and sharp anomaly on the DSC curve no. 5).

At heating of the sample c from 298 to 403 K with a scanning rate of 20 K/min gives the DSC curve no. 6 presented in Fig. 4. At the temperature range of 298–370 K we can see a very small anomaly at T^{h}_{C2} connected with the phase transition: stable phase KIb → stable phase KIa and one big anomaly at T^{h}_{C1} connected with the phase transition: phase KIa → phase K0. Later, while heating hermetically closed sample c, being in the K0 phase, up to 403 K, experiences a phase transition at $T_{m1} = 389$ K into the phase named L0. This phase transition is connected with partial melting of $[Zn(DMSO)_6](ClO_4)_2$ and is connected with a broad anomaly on DCS curve no. 6 and with entropy change $\Delta S \approx 19\ J\ mol^{-1}\ K^{-1}$. As can be see in Fig. 4 (DSC curve no. 7) while cooling the sample from partially liquid phase L0, with a scanning rate of 15 K/min, it crystallizes at 396 K into the K0 phase. On further cooling, phase K0 is supercooled and just at 309 K the K0′ phase transforms into the metastable phase KII (see Fig. 4 and compare with Fig. 3). Next, the second new heating of the sample c with a scanning rate of 10 K/min gives a somewhat different picture of the phase transformation, which can be seen on the DSC curve no. 8 (see Fig. 4). When the sample is heated up, the phase transition occurs from metastable

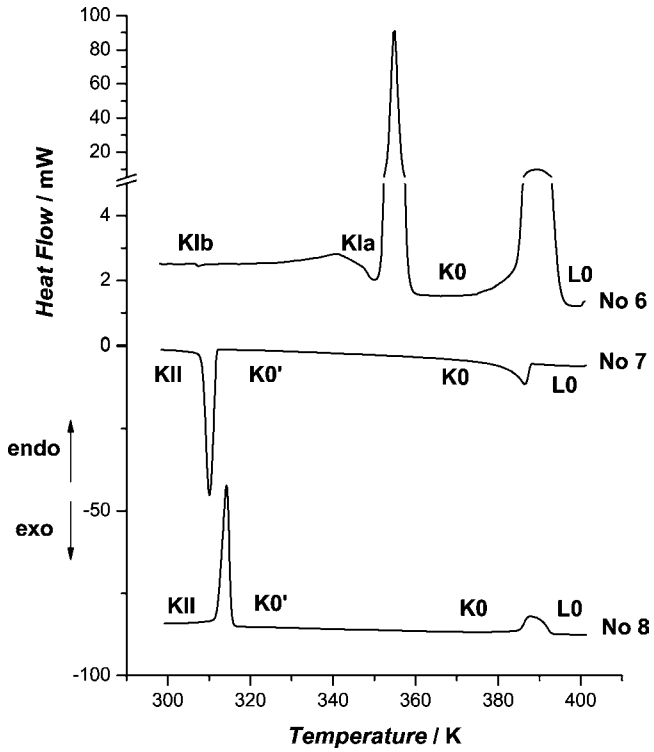

Fig. 4. DSC curves obtained for $[Zn(DMSO)_6](ClO_4)_2$ during heating with a scanning rate of 20 K/min (curve no. 6), during cooling with a scanning rate of 15 K/min (curve no. 7) and during heating at 298–403 with a scanning rate of 10 K/min (curve no. 8). Sample c = 17.94 mg.

KII phase to supercooled K0 phase at T^{h}_{C1}. Later, the K0 phase experiences a phase transition at T_{m1} into the L0 phase.

As we can see in Fig. 5 (DSC curve no. 9), the next cooling sample c with a scanning rate of 10 K/min gives an identical phase transformation picture to that which was presented in Fig. 4. While cooling the sample from 403 K, being in L0 phase it undergoes phase transition to K0 phase that is connected with re-crystallization of HZnC. On further cooling, the K0 phase becomes deeply supercooled, and then supercooled K0 phase (phase K0′) experiences the phase transition at ca. 310 K into a metastable phase KII. Next the third heating of the sample c with a scanning rate of 15 K/min gives the DSC curve no. 10 presented in Fig. 5. The sample in the metastable phase KII converts at the exothermic process to the stable phase KIb (small and broad exothermic anomaly at ca. 270 K). Later there is a very small anomaly connected with the phase transition from KIb to KIa at T^{h}_{C2}. On further heating the stable phase KIa endothermically converts at T^{h}_{C1} into the stable phase K0. In the end, the stable K0 phase partially melts to the L0 at T_{m2}.

It is not possible to determine the nature of the observed phases only on the basis of DSC measurements. The measurements by complementary methods, like for example X-ray diffraction, are now in progress. However, using a microscope we have observed that phases KIa, KIb and K0 were the solid phases and L0 is partially melted phase. Taking into account the findings from thermal analysis we can postulate that at T_{m2} the sample became partially dissolved in DMSO, which arises out of a decomposition of $[Zn(DMSO)_6](ClO_4)_2$

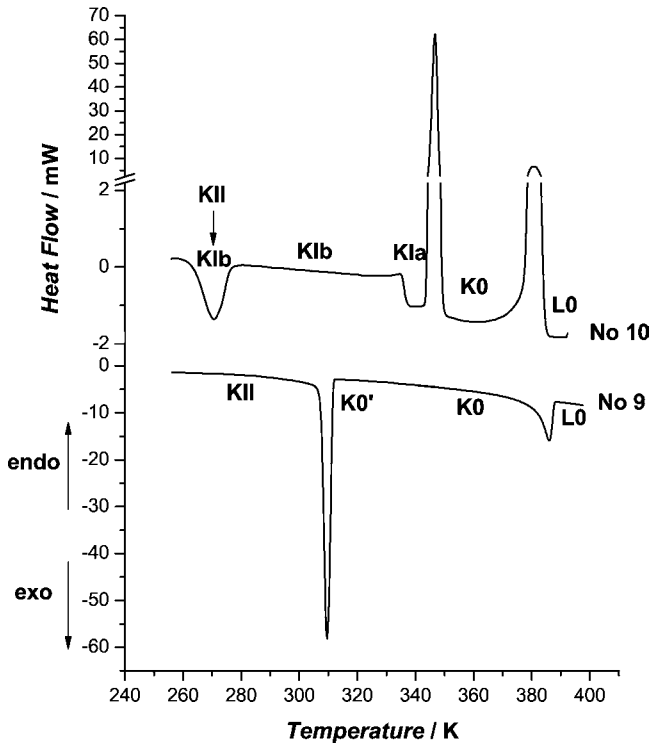

Fig. 5. DSC curves obtained for $[Zn(DMSO)_6](ClO_4)_2$ during cooling (curve no. 9) from 403 to 250 K and during heating at 250–403 K (curve no. 10) with a scanning rate of 15 K/min. Sample c = 17.94 mg.

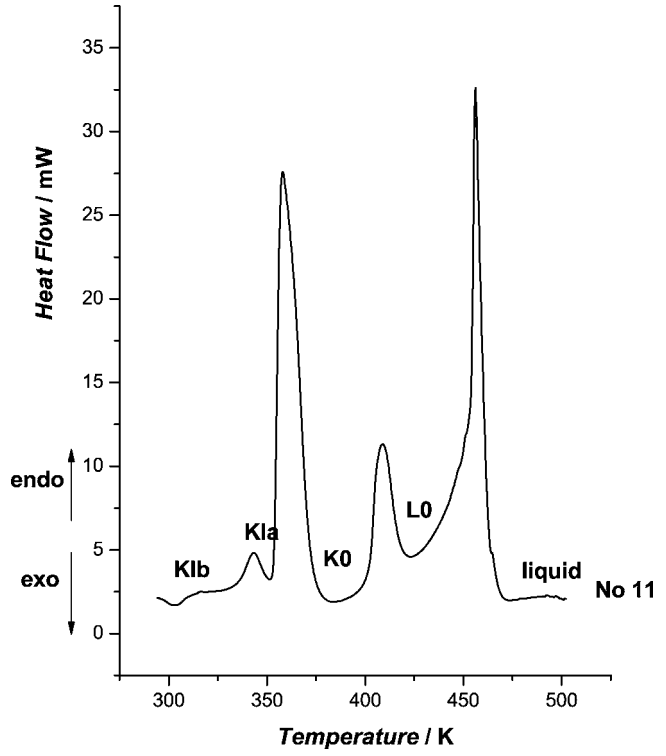

Fig. 6. DSC curve obtained at the temperature range of 283–513 K during heating of $[Zn(DMSO)_6](ClO_4)_2$ with a scanning rate of 20 K/min (curve no. 11). Sample d = 28.34 mg.

to $[Zn(DMSO)_5](ClO_4)_2$ (compare Section 2.2), because the sample is at this DSC experiment hermetically closed in the calorimetric vessel. Moreover, it was concluded from the change of the entropy of transitions ΔS (see Table 2) that phases K0 and supercooled K0 are more likely to be orientationally dynamically disordered crystals, the so called "ODIC" or "ODDIC". The $\Delta S_{m1} = 47.0\,J\,K^{-1}\,mol^{-1}$ connected with the melting is low but does not fulfill the Timmermans' criterion [12] for plastic crystals ($\Delta S < 24\,J\,K^{-1}\,mol^{-1}$). Phases KIa, KIb and KII are more or less ordered ones. It can be deduced from the small values of $\Delta S \approx 7\,J\,K^{-1}\,mol^{-1}$ connected with KIb ↔ KIa phase transition at T^{h}_{C2}, and from the big values of $\Delta S \approx 71\,J\,K^{-1}\,mol^{-1}$ and $\Delta S \approx 68\,J\,K^{-1}\,mol^{-1}$ connected with phase transitions: KIa ↔ K0 at T^{h}_{C1} and KII ↔ K0′ at T^{h}_{C3}, respectively (see Table 2).

While heating up the sample *d* above the T^{h}_{C1} temperature, it completely melts at $T_{m1} = 465\,K$ with $\Delta S = 47\,J\,mol^{-1}\,K^{-1}$, which is not at all as large value as for most melting processes of ionic crystals. However, as we just stated above, because this value is twice as large as that resulting from Timmermans' criterion [12], phase K0 cannot be named a rotational phase. The DSC curve showing the anomaly resulting from the melting process can be seen in Fig. 6 (curve no. 11).

Acknowledgements

Our thanks are due to Professor S. Wróbel from the Faculty of Physics, Astronomy and Applied Computer Science, Jagiellonian University, for enabling us to perform the DSC measurements. We are grateful also to Dr. Hab. E. Mikuli from the Faculty of Chemistry, Jagiellonian University, for stimulating the discussion. We are also grateful to J. Ściesiński MSc and Dr. Hab. E. Ściesińska from H. Niewodniczański Institute of Nuclear Physics, PAS, in Kraków, for recording for us the FT-FIR spectrum. We are also very obliged to Dr. Hab. A. Wesełucha-Birczyńska and Dr. M. Molenda, both from the Regional Laboratory of Physicochemical Analysis and Structural Research in Kraków, for recording the FT-RS spectrum and for DSC, TG, DTA measurements, respectively.

Appendix A. Supplementary data

Supplementary data associated with this article can be found, in the online version, at doi:10.1016/j.tca.2006.02.005.

References

[1] I. Persson, Acta Chem. Scand. A 36 (1982) 7.
[2] M. Calligaris, O. Carugo, Coord. Chem. Rev. 153 (1996) 83.
[3] M. Sandström, I. Persson, S. Ahrland, Acta Chem. Scand. A 32 (1978) 607.
[4] A. Migdał-Mikuli, E. Mikuli, E. Szostak, J. Serwońska, Z. Naturforsch. 58a (2003) 341.
[5] A. Migdał-Mikuli, E. Szostak, Thermochim. Acta 426 (2005) 191.
[6] A. Migdał-Mikuli, E. Szostak, Z. Naturforsch. 60a (2005) 289.
[7] F.A. Cotton, R. Francis, J. Am. Chem. Soc. 82 (1960) 2986.
[8] K. Nakamoto, Infrared and Raman Spectra of Inorganic and Coordination Compounds, Part B, 5th ed., A. Wiley Intersience Publ., NY, 1997.
[9] Raman/IR Atlas, Verlag Chemie GmbH, Weinheim, Bergstr., 1974.
[10] A. Migdał-Mikuli, E. Mikuli, S. Wróbel, Ł. Hetmańczyk, Z. Naturforsch. 54a (1999) 590.
[11] Y. Mnyukh, Fundamentals of Solid-State Phase Transitions, Ferromagnetism and Ferroelectricity, 1st Books Library, 2001.
[12] J. Timmermans, J. Phys. Chem. Solids 18 (1961) 1.